Acta Cryst E CRYSTALLOGRAPHIC COMMUNICATIONS

ISSN 2056-9890

Crystal structure and Hirshfeld surface analysis of aqua(1*H*-imidazole-κN^3)[*N*-(2-oxidobenzylidene) threonato-$\kappa^3 O,N,O'$]zinc(II)

Fumishi Yoshizawa, Anna Okui, Daisuke Nakane and Takashiro Akitsu*

Department of Chemistry, Faculty of Science, Tokyo University of Science, 1-3, Kagurazaka, Shinjuku-ku, Tokyo 162-8601, Japan. *Correspondence e-mail: akitsu2@rs.tus.ac.jp

Received 18 February 2025
Accepted 16 March 2025

Edited by Y. Ozawa, University of Hyogo, Japan

Keywords: Schiff base ligand; zinc(II) complex; amino acid; Hirshfeld surface analysis; crystal structure.

CCDC reference: 2431599

Supporting information: this article has supporting information at journals.iucr.org/e

The title complex, $[Zn(C_{11}H_{11}NO_4)(C_3H_4N_2)(H_2O)]$, which includes a tridentate ligand, was synthesized from L-threonine and salicylaldehyde. One water molecule and one imidazole molecule additionally coordinate the zinc(II) center in a distorted trigonal–bipyramidal geometry. The crystal structure features N—H···O and O—H···O hydrogen bonds. A Hirshfeld surface analysis indicates that the most important contributions to the packing are from H···H/H···H (50.7%) and O···H/H···O (25.0%) contacts.

1. Chemical context

Amino acid Schiff bases have an azomethine (C═N) group synthesized by mixing primary amines and formyls, and are used as organic ligands (Katsuumi *et al.*, 2020; Hirotsu *et al.*, 2022; Gozdas *et al.*, 2024; Bowman *et al.*, 2021). According to a review on the synthesis of amino acid Schiff base–metal complexes (Akitsu *et al.*, 2022), in general, Schiff bases and their metal complexes are versatile compounds and are widely used in many research and industrial applications. For example, supramolecular encapsulation of nanocrystalline Schiff bases in *β*-cyclodextrin (Mahato *et al.*, 2022), photoreaction with titanium dioxide (Takeshita & Akitsu, 2015), photocatalytic reduction of hexavalent chromium (Nakagame *et al.*, 2019; Miyagawa *et al.*, 2020), Schiff base ligand–SPCE (screen-printed carbon electrode) sensors (Bressi *et al.*, 2022), and flexible ruthenium(II) Schiff base complexes, which have been shown to play a key role in drug activity upon photoirradiation (Gillard *et al.*, 2020).

Furthermore, Schiff base complexes are considered an important class of organic compounds with a wide range of biological properties, including free-radical-scavenging activity, antibacterial activity, and antitumor activity (Kumar, 2022). In our laboratory, we synthesized novel mono-chlorinated Schiff base copper(II) complexes and tested their antibacterial activity against Gram-positive and Gram-negative bacteria. The most active compounds were then tested for antioxidant activity, and it was found that *E. coli* absorbed these compounds with very high affinity (Otani *et al.*, 2022). We are also conducting research using microfluidic devices to efficiently synthesize amino acid Schiff base copper(II) complexes (Kobayashi *et al.*, 2023), and synthesis of amino acid Schiff base copper(II) complexes containing azobenzene moiety (Kaneda *et al.*, 2024). Our goal is to evaluate the SOD activity of artificial metalloproteins made by conjugating these Schiff base copper(II) complexes with proteins such as lysozyme (Furuya *et al.*, 2023; Nakane *et al.*, 2024).

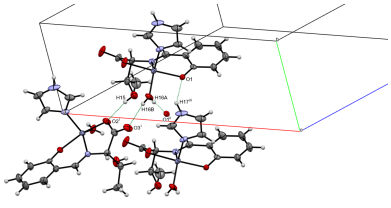

Therefore, we have been studying the bioactivity of Schiff base complexes derived from amino acids and decided to synthesize a zinc complex of this ligand to compare its bioactivity with that of the copper complex. In this report, we describe the crystal structure and intermolecular interactions of the zinc(II) complex, coordinated with imidazole as a model for histidine residues in proteins.

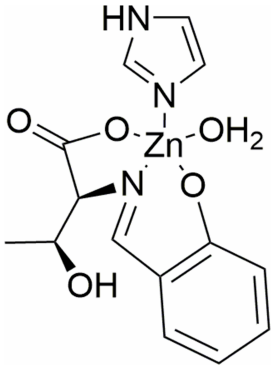

2. Structural commentary

The molecular structure of the title compound consists of one imidazole molecule, one water molecule and a tridentate ligand, which is synthesized from L-threonine and salicylaldehyde, coordinating to a zinc(II) center in distorted trigonal–bipyramidal geometry (Fig. 1). The two largest coordination angles O1—Zn01—O2 and N1—Zn01—O5 are 166.60 (11), 130.65 (13)°, and the τ value derived from them, which is five-coordinated geometry index, is 0.599 (Addison *et al.*, 1984). The C7—N1 distance is 1.276 (5) Å, which is close to a typical C=N double-bond length for an imine (Katsuumi *et al.*, 2020). The Zn01—O1, Zn01—O2 and Zn01—O5 coordination lengths are 2.061 (2), 2.117 (3) and 1.996 (3) Å, respectively, close to a typical Zn—O bond length (Noor *et al.*, 2021). The Zn01—N1 and Zn1—N2 bonds of 2.038 (3) and 2.015 (3) Å corresponds to a typical Zn—N bond length (Noor *et al.*, 2021). These five atoms coordinating to Zn1 have similar bond distances.

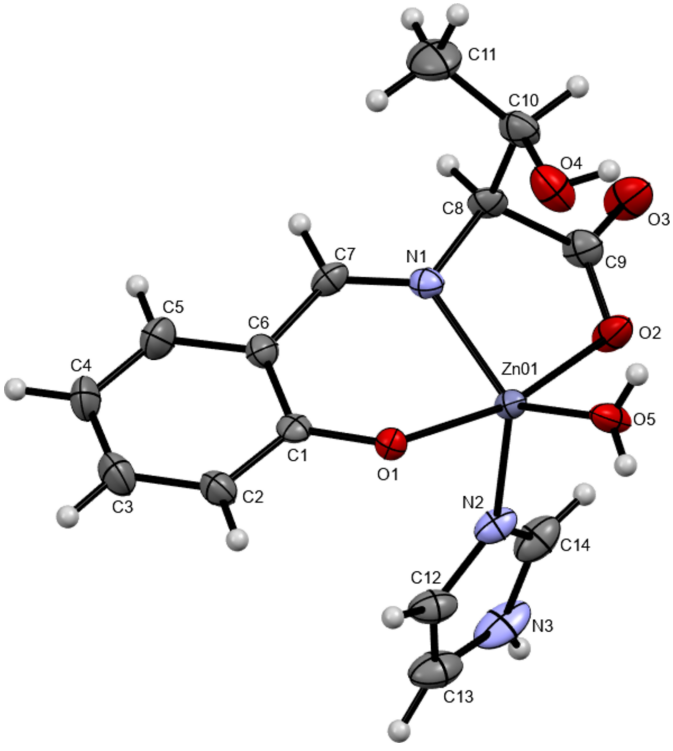

Figure 1
The molecular structure of the title compound with ellipsoids drawn at the 50% probability level.

Table 1
Hydrogen-bond geometry (Å, °).

D—H···A	D—H	H···A	D···A	D—H···A
O4—H15···O2^{i}	0.79 (7)	1.89 (7)	2.678 (4)	170 (8)
O5—H16A···O1^{ii}	0.79 (7)	1.91 (7)	2.708 (4)	178 (6)
O5—H16B···O3^{i}	0.72 (8)	2.02 (8)	2.724 (4)	165 (7)
N3—H17···O1^{iii}	0.88	2.06	2.830 (6)	145

Symmetry codes: (i) $-x+\frac{3}{2}, y-\frac{1}{2}, -z$; (ii) $-x+1, y, -z$; (iii) $x, y+1, z$.

3. Supramolecular features

Four intermolecular hydrogen bonds are observed in the crystal (Fig. 2); two hydrogen bonds (O5—H16A···O1 and O5H—H16B···O3) lead to the formation of a chain structure along the a-axis direction. One hydrogen bond (O4—H15···O2) is formed along the c-axis direction (Table 1). In addition, an intermolecular N3—H17···O1 interaction is found (symmetry codes given in Table 1).

A Hirshfeld surface analysis (McKinnon *et al.*, 2007; Spackman & Jayatilaka, 2009) was performed to further investigate the intermolecular interactions and contacts. The intermolecular O—H···O hydrogen bonds are indicated by bright red spots appearing near O on the Hirshfeld surfaces mapped over d_{norm} and by two sharp spikes of almost the same length in the region 1.6 Å < (d_e + d_i) < 2.0 Å in the 2D fingerprint plots (Fig. 3).

The contributions to the packing from H···H, C···C, C···H/H···C, N···H/H···N, and H···O/O···H contacts are

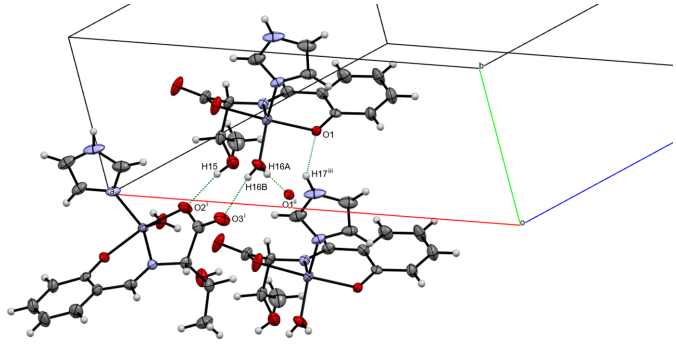

Figure 2
A view of the O—H···O and N—H···O hydrogen bonds, shown as dashed lines. [Symmetry codes: (i) $-x+\frac{3}{2}, y-\frac{1}{2}, -z$; (ii) $-x+1, y, -z$; (iii) $x, y+1, z$.]

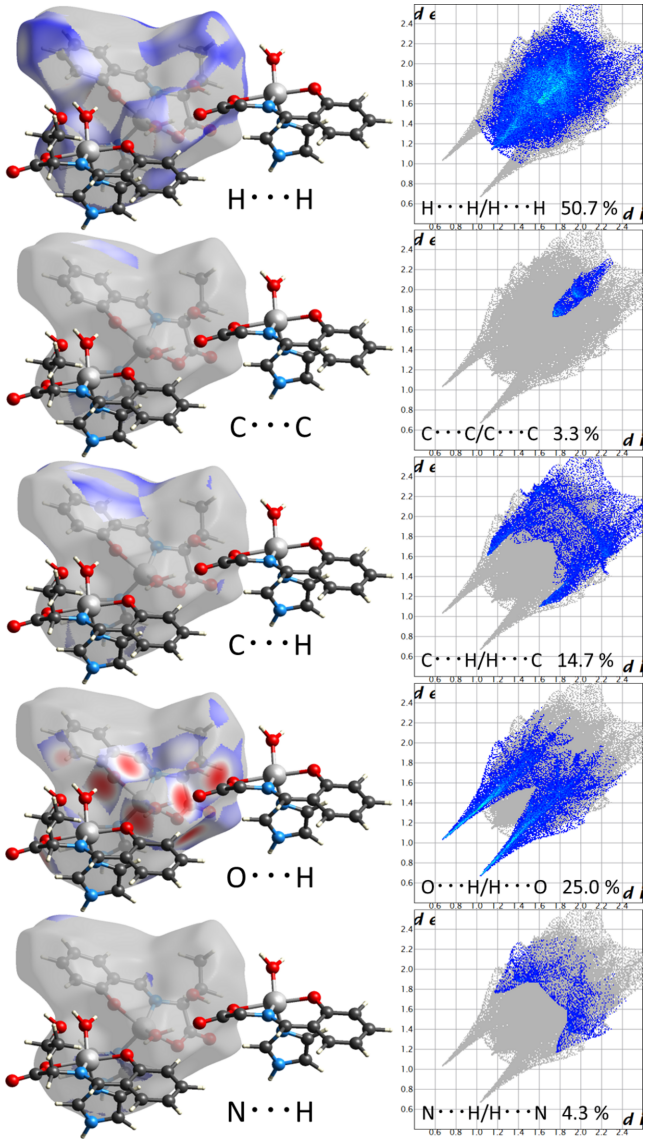

Figure 3
Hirshfeld surfaces mapped over d_{norm} and the two-dimensional fingerprint plots.

50.7, 3.3, 14.9, 4.3 and 25.0%, respectively. The structure is characterized by high proportion of H···H interactions, where H···H are van der Waals interactions. The high value of C···H/H···C is thought to arise from C—H···π interactions due to the presence of aromatic rings in the compound. The low value of C···C is the result of the low contribution of π–π stacking due to non-overlapping aromatic rings in the structure.

4. Database survey

A search in the Cambridge Structural Database (CSD, Version 5.43, update of November 2021; Groom *et al.*, 2016) for similar structures returned four relevant entries: aqua-[*N*-{[2-oxyphenyl]methylidene}threoninato]-(methanol)copper(II) (YUYFUW; Katsuumi *et al.*, 2020), oxonium bis{2-[(tetrahydrofuran-2-ylmethyl)carbonoimidoyl]phenolato}zinc(II) perchlorate (KOVRAQ; Mandal *et al.*, 2014), (3-(4-hydroxyphenyl)-2-{[(2-oxidophenyl)methylidene]amino}propanoato)-(1*H*-imidazole)copper(II) (GIQWUC; Suzuki *et al.*, 2023), mono/bis(aqua-κO)[*N*-(2-oxidobenzylidene)valinato-$\kappa^3 O,N,O'$]copper(II) (VEXZIL; Akiyama *et al.*, 2023).

Table 2
Experimental details.

Crystal data	
Chemical formula	$[Zn(C_{11}H_{11}NO_4)(C_3H_4N_2)(H_2O)]$
M_r	372.67
Crystal system, space group	Monoclinic, *C*2
Temperature (K)	173
a, *b*, *c* (Å)	18.3835 (7), 7.7141 (3), 13.3800 (5)
β (°)	123.787 (1)
V (Å^3)	1576.99 (11)
Z	4
Radiation type	Mo $K\alpha$
μ (mm^{-1})	1.59
Crystal size (mm)	0.10 × 0.10 × 0.10
Data collection	
Diffractometer	Bruker-AXS D8 QUEST
Absorption correction	Multi-scan
T_{min}, T_{max}	0.64, 0.86
No. of measured, independent and observed [$I > 2\sigma(I)$] reflections	10846, 2752, 2701
R_{int}	0.073
$(\sin\theta/\lambda)_{max}$ (Å^{-1})	0.596
Refinement	
$R[F^2 > 2\sigma(F^2)]$, $wR(F^2)$, *S*	0.032, 0.074, 1.07
No. of reflections	2752
No. of parameters	218
No. of restraints	1
H-atom treatment	H atoms treated by a mixture of independent and constrained refinement
$\Delta\rho_{max}$, $\Delta\rho_{min}$ (e Å^{-3})	0.35, −0.29
Absolute structure	Flack *x* determined using 1180 quotients $[(I^+)-(I^-)]/[(I^+)+(I^-)]$ (Parsons *et al.*, 2013)
Absolute structure parameter	0.143 (11)

Computer programs: *APEX2* and *SAINT* (Bruker, 2019), *SHELXT2018/2* (Sheldrick, 2015*a*), *SHELXL2019/1* (Sheldrick, 2015*b*) and *ShelXle* (Hübschle *et al.*, 2011).

5. Synthesis and crystallization

L-threonine (11.912 mg, 0.10 mmol) was reacted with salicylaldehyde (12.212 mg, 0.10 mmol) in methanol (5 mL) and water (2 mL), and the resulting mixture was stirred at 313 K for 1 h to afford a yellow solution. To this solution, zinc(II) acetate dihydrate (21.951 mg, 0.100 mmol) was added and it was stirred at 313 K for 1 h. Then imidazole (6.808 mg, 0.10 mmol) was added, yielding a pale-yellow solution. For crystallization, the solution was placed in air at 300 K for several days, and the title complex was obtained as pale yellow columnar-shaped single crystals suitable for single-crystal X-ray diffraction structure analysis. All reagents are commercially available, but L-threonine moiety may partially racemize during synthesis. IR (ATR): 1070 cm^{-1}(*w*), 1284 cm^{-1}(*m*), 1376 cm^{-1}(*m*), 1473 cm^{-1}(*m*), 1475 cm^{-1}(*m*), 1548 cm^{-1}(*w*, C═C double bond), 1622 cm^{-1}(*s*, C═O double bond), 1634 cm^{-1}(*s*, C═N double bond), 3251 cm^{-1}(*br*,

O—H). UV-vis (H_2O): 270 nm (ε = 38000 L mol^{-1} cm^{-1}, π–π*); 359 nm (ε = 18000 L mol^{-1} cm^{-1}, n–π*).

6. Refinement

Crystal data, data collection and structure refinement details are summarized in Table 2. All C-bound H atoms were placed in geometrically calculated positions (C—H = 0.94–1.00 Å) and were constrained using a riding model with U_{iso}(H) = 1.2U_{eq}(C) for R_2CH and R_3CH H atoms and 1.5U_{eq}(C) for the methyl H atoms. The N-bound H atom H17 was constrained using a riding model with U_{iso}(H) = 1.2U_{eq}(N), and the O-bound H atoms H15, H16*A*, H16*B* were located based on a difference-Fourier map and refined freely.

Funding information

Funding for this research was provided by: Grant-in-Aid for Scientific Research (B) KAKENHI (24K00912).

References

Addison, A. W., Rao, T. N., Reedijk, J., van Rijn, J. & Verschoor, G. C. (1984). *J. Chem. Soc. Dalton Trans.* pp. 1349–1356.
Akitsu, T., Miroslaw, B. & Sudarsan, S. (2022). *Int. J. Mol. Sci.* **23**, 10005.
Akiyama, Y., Suzuki, S., Suda, S., Takiguchi, Y., Nakane, D. & Akitsu, T. (2023). *Acta Cryst.* E**79**, 361–366.
Bowman, E. A., England, B. L., Patterson, M. A., Price, N. S., Stepler, K. E., Curnutte, H. A., Lease, R. E., Bradley, C. A. & Craig, P. R. (2021). *Inorg. Chim. Acta*, **524**, 120415.
Bressi, V., Akbari, Z., Montazerozohori, M., Ferlazzo, A., Iannazzo, D., Espro, C. & Neri, G. (2022). *Sensors* **22**, 900.
Bruker (2019). *APEX2* and *SAINT*. Bruker Nano Inc., Madison, Wisconsin, USA.
Furuya, T., Nakane, D., Kitanishi, K., Katsuumi, N., Tsaturyan, A., Shcherbakov, I. N., Unno, M. & Akitsu, T. (2023). *Sci. Rep.* **13**, 6892.
Gillard, M., Weynand, J., Bonnet, H., Loiseau, F., Decottignies, A., Dejeu, J., Defrancq, E. & Elias, B. (2020). *Chem. A Eur. J.* **26**, 13849–13860.
Gozdas, S., Kose, M., Mckee, V., Elmastas, M., Demirtas, I. & Kurtoglu, M. (2024). *J. Mol. Struct.* **1304**, 137691.
Groom, C. R., Bruno, I. J., Lightfoot, M. P. & Ward, S. C. (2016). *Acta Cryst.* B**72**, 171–179.
Hirotsu, M., Sanou, J., Nakae, T., Matsunaga, T. & Kinoshita, I. (2022). *Acta Cryst.* E**78**, 500–505.
Hübschle, C. B., Sheldrick, G. M. & Dittrich, B. (2011). *J. Appl. Cryst.* **44**, 1281–1284.
Kaneda, A., Suzuki, S., Nakane, D., Kashiwagi, Y. & Akitsu, T. (2024). *Acta Cryst.* E**80**, 468–471.
Katsuumi, N., Onami, Y., Pradhan, S., Haraguchi, T. & Akitsu, T. (2020). *Acta Cryst.* E**76**, 1539–1542.
Kobayashi, M., Akitsu, T., Furuya, M., Sekiguchi, T., Shoji, S., Tanii, T. & Tanaka, D. (2023). *Micromachines* **14**, 890.
Kumar, K. S. (2022). *Results Chem.* **4**, 100463.
Mahato, R. K., Debnath, A., Das, A., Sarkar, D., Bhattacharyya, S. & Biswas, B. (2022). *Carbohydr. Polym.* **291**, 119614.
Mandal, H., Chakrabartty, S. & Ray, D. (2014). *RSC Adv.* **4**, 65044–65055.
McKinnon, J. J., Jayatilaka, D. & Spackman, M. A. (2007). *Chem. Commun.* pp. 3814–3816.
Miyagawa, Y., Tsatsuryan, A., Haraguchi, T., Shcherbakov, I. & Akitsu, T. (2020). *New J. Chem.* **44**, 16665–16674.
Nakagame, R., Tsaturyan, A., Haraguchi, T., Pimonova, Y., Lastovina, T., Akitsu, T. & Shcherbakov, I. (2019). *Inorg. Chim. Acta*, **486**, 221–231.
Nakane, D., Akiyama, Y., Suzuki, S., Miyazaki, R. & Akitsu, T. (2024). *Front. Chem.* **11**, 1330833.
Noor, S., Suda, S., Haraguchi, T., Khatoon, F. & Akitsu, T. (2021). *Acta Cryst.* E**77**, 542–546.
Otani, N., Fayeulle, A., Nakane, D., Léonard, E. & Akitsu, T. (2022). *Appl. Microbiol.* **2**, 438–448.
Parsons, S., Flack, H. D. & Wagner, T. (2013). *Acta Cryst.* B**69**, 249–259.
Sheldrick, G. M. (2015*a*). *Acta Cryst.* A**71**, 3–8.
Sheldrick, G. M. (2015*b*). *Acta Cryst.* C**71**, 3–8.
Spackman, M. A. & Jayatilaka, D. (2009). *CrystEngComm*, **11**, 19–32.
Suzuki, S., Akiyama, Y., Nakane, D. & Akitsu, T. (2023). *Acta Cryst.* E**79**, 596–599.
Takeshita, Y. & Akitsu, T. (2015). *Pure Appl. Chem.* **3**, 11–17.

supporting information

Acta Cryst. (2025). E**81**, 332-335 [https://doi.org/10.1107/S2056989025002385]

Crystal structure and Hirshfeld surface analysis of aqua(1*H*-imidazole-κN^3)[*N*-(2-oxidobenzylidene)threonato-$\kappa^3 O,N,O'$]zinc(II)

Fumishi Yoshizawa, Anna Okui, Daisuke Nakane and Takashiro Akitsu

Computing details

Aqua(1*H*-imidazole-κN^3)[*N*-(2-oxidobenzylidene)threonato-$\kappa^3 O,N,O'$]zinc(II)

Crystal data

$[Zn(C_{11}H_{11}NO_4)(C_3H_4N_2)(H_2O)]$
M_r = 372.67
Monoclinic, *C*2
a = 18.3835 (7) Å
b = 7.7141 (3) Å
c = 13.3800 (5) Å
β = 123.787 (1)°
V = 1576.99 (11) Å^3
Z = 4
F(000) = 768
D_x = 1.570 Mg m^{-3}
Mo *K*α radiation, λ = 0.71073 Å
Cell parameters from 6515 reflections
θ = 3.0–25.0°
μ = 1.59 mm^{-1}
T = 173 K
Prism, yellow
0.10 × 0.10 × 0.10 mm

Data collection

Bruker-AXS D8 QUEST diffractometer
Detector resolution: 7.3910 pixels mm^{-1}
profile data from θ/2θ scans
Absorption correction: multi-scan
T_{min} = 0.64, T_{max} = 0.86
10846 measured reflections
2752 independent reflections
2701 reflections with $I > 2\sigma(I)$
R_{int} = 0.073
θ_{max} = 25.1°, θ_{min} = 3.0°
h = −21→21
k = −9→9
l = −15→15

Refinement

Refinement on F^2
Least-squares matrix: full
$R[F^2 > 2\sigma(F^2)]$ = 0.032
$wR(F^2)$ = 0.074
S = 1.07
2752 reflections
218 parameters
1 restraint
Hydrogen site location: mixed
H atoms treated by a mixture of independent and constrained refinement
$w = 1/[\sigma^2(F_o^2) + (0.0364P)^2]$ where $P = (F_o^2 + 2F_c^2)/3$
$(\Delta/\sigma)_{max} < 0.001$
$\Delta\rho_{max}$ = 0.35 e Å^{-3}
$\Delta\rho_{min}$ = −0.29 e Å^{-3}
Absolute structure: Flack *x* determined using 1180 quotients $[(I^+)-(I^-)]/[(I^+)+(I^-)]$ (Parsons *et al.*, 2013)
Absolute structure parameter: 0.143 (11)

Special details

Geometry. All esds (except the esd in the dihedral angle between two l.s. planes) are estimated using the full covariance matrix. The cell esds are taken into account individually in the estimation of esds in distances, angles and torsion angles; correlations between esds in cell parameters are only used when they are defined by crystal symmetry. An approximate (isotropic) treatment of cell esds is used for estimating esds involving l.s. planes.

Fractional atomic coordinates and isotropic or equivalent isotropic displacement parameters (Å²)

	x	*y*	*z*	U_{iso}*/U_{eq}
Zn01	0.65438 (2)	0.42759 (7)	0.11898 (3)	0.01670 (17)
O1	0.59603 (16)	0.2984 (3)	0.1916 (2)	0.0174 (5)
O2	0.74153 (18)	0.5370 (4)	0.0799 (3)	0.0323 (7)
O3	0.8834 (2)	0.5634 (5)	0.1533 (3)	0.0391 (8)
O4	0.7676 (2)	0.1327 (5)	0.1191 (3)	0.0372 (8)
O5	0.5804 (2)	0.3045 (4)	−0.0380 (3)	0.0276 (7)
H16A	0.529 (5)	0.302 (8)	−0.085 (6)	0.041000*
N1	0.7722 (2)	0.3625 (4)	0.2698 (3)	0.0196 (7)
N2	0.6124 (2)	0.6638 (4)	0.1298 (3)	0.0241 (7)
N3	0.6028 (3)	0.9438 (6)	0.1430 (3)	0.0420 (10)
H17	0.611949	1.055498	0.141612	0.050000*
H15	0.768 (5)	0.115 (10)	0.061 (6)	0.063000*
C1	0.6293 (2)	0.2935 (5)	0.3089 (3)	0.0187 (7)
C2	0.5734 (3)	0.2624 (6)	0.3481 (4)	0.0273 (9)
H2	0.512602	0.246220	0.290352	0.033000*
C3	0.6056 (3)	0.2549 (7)	0.4692 (4)	0.0365 (11)
H3	0.566229	0.235803	0.492934	0.044000*
C4	0.6946 (3)	0.2747 (7)	0.5573 (4)	0.0372 (11)
H4	0.716190	0.269067	0.640331	0.045000*
C5	0.7501 (3)	0.3026 (7)	0.5208 (4)	0.0339 (10)
H5	0.810969	0.314747	0.580187	0.041000*
C6	0.7204 (3)	0.3139 (5)	0.3988 (3)	0.0221 (8)
C7	0.7866 (3)	0.3359 (6)	0.3735 (3)	0.0230 (8)
H7	0.845966	0.330118	0.439697	0.028000*
C8	0.8438 (2)	0.3703 (5)	0.2529 (3)	0.0225 (8)
H8	0.899618	0.402041	0.330026	0.027000*
C9	0.8220 (3)	0.5031 (6)	0.1559 (4)	0.0268 (9)
C10	0.8523 (3)	0.1890 (6)	0.2094 (4)	0.0297 (9)
H10	0.887625	0.201059	0.173851	0.036000*
C11	0.8964 (4)	0.0585 (8)	0.3105 (6)	0.0507 (14)
H11A	0.955393	0.099246	0.372280	0.076000*
H11B	0.900354	−0.053288	0.279021	0.076000*
H11C	0.862170	0.045004	0.345727	0.076000*
C12	0.5546 (3)	0.6991 (6)	0.1608 (4)	0.0295 (9)
H12	0.523720	0.613729	0.174295	0.035000*
C13	0.5472 (3)	0.8718 (6)	0.1695 (4)	0.0381 (11)
H13	0.511549	0.930343	0.189603	0.046000*
C14	0.6408 (3)	0.8169 (7)	0.1196 (4)	0.0346 (10)
H14	0.681965	0.833681	0.098842	0.041000*

H16B	0.599 (5)	0.243 (10)	−0.059 (6)	0.052000*

Atomic displacement parameters (Å²)

	U^{11}	U^{22}	U^{33}	U^{12}	U^{13}	U^{23}
Zn01	0.0144 (2)	0.0149 (2)	0.0197 (2)	−0.00040 (18)	0.00884 (17)	0.00248 (17)
O1	0.0165 (12)	0.0172 (13)	0.0178 (11)	−0.0024 (11)	0.0091 (10)	−0.0005 (10)
O2	0.0171 (14)	0.0431 (19)	0.0350 (15)	0.0022 (13)	0.0133 (12)	0.0193 (14)
O3	0.0215 (15)	0.045 (2)	0.0486 (18)	−0.0046 (14)	0.0184 (13)	0.0176 (16)
O4	0.0358 (17)	0.045 (2)	0.0399 (17)	−0.0091 (15)	0.0269 (15)	−0.0134 (16)
O5	0.0164 (14)	0.0383 (19)	0.0231 (14)	0.0040 (14)	0.0080 (12)	−0.0115 (13)
N1	0.0190 (15)	0.0173 (14)	0.0238 (15)	0.0012 (13)	0.0127 (13)	0.0015 (12)
N2	0.0222 (16)	0.0146 (17)	0.0257 (16)	−0.0017 (13)	0.0073 (13)	0.0010 (13)
N3	0.048 (2)	0.0124 (18)	0.0373 (18)	0.0022 (19)	0.0066 (16)	−0.0011 (18)
C1	0.0222 (18)	0.0121 (17)	0.0214 (17)	0.0030 (15)	0.0119 (15)	−0.0014 (14)
C2	0.025 (2)	0.034 (2)	0.029 (2)	0.0011 (18)	0.0186 (17)	−0.0006 (18)
C3	0.037 (2)	0.050 (3)	0.034 (2)	0.002 (2)	0.027 (2)	0.001 (2)
C4	0.038 (2)	0.057 (3)	0.0196 (19)	0.007 (2)	0.0182 (18)	0.002 (2)
C5	0.030 (2)	0.045 (3)	0.0198 (19)	0.004 (2)	0.0099 (17)	0.0006 (19)
C6	0.0226 (18)	0.024 (2)	0.0195 (17)	0.0026 (16)	0.0113 (15)	−0.0012 (15)
C7	0.0178 (17)	0.024 (2)	0.0192 (18)	0.0008 (15)	0.0053 (15)	0.0020 (15)
C8	0.0116 (16)	0.027 (2)	0.0259 (18)	−0.0022 (15)	0.0085 (15)	0.0012 (15)
C9	0.022 (2)	0.026 (2)	0.034 (2)	−0.0045 (18)	0.0170 (18)	0.0028 (18)
C10	0.025 (2)	0.033 (2)	0.039 (2)	0.0010 (18)	0.0230 (19)	0.0036 (19)
C11	0.062 (3)	0.036 (3)	0.066 (3)	0.023 (3)	0.042 (3)	0.018 (3)
C12	0.024 (2)	0.021 (2)	0.033 (2)	0.0022 (17)	0.0095 (18)	−0.0052 (17)
C13	0.035 (2)	0.026 (2)	0.039 (2)	0.0076 (18)	0.0116 (19)	−0.0052 (18)
C14	0.036 (2)	0.023 (3)	0.030 (2)	−0.003 (2)	0.0088 (19)	0.0024 (17)

Geometric parameters (Å, º)

Zn01—O5	1.996 (3)	N3—C14	1.337 (7)
Zn01—N2	2.015 (3)	N3—C13	1.371 (7)
Zn01—N1	2.038 (3)	C1—C2	1.410 (6)
Zn01—O1	2.060 (2)	C1—C6	1.427 (5)
Zn01—O2	2.117 (3)	C2—C3	1.383 (6)
O1—C1	1.331 (4)	C3—C4	1.394 (7)
O2—C9	1.272 (5)	C4—C5	1.371 (7)
O3—C9	1.238 (5)	C5—C6	1.407 (6)
O4—C10	1.408 (6)	C6—C7	1.443 (6)
N1—C7	1.276 (5)	C8—C9	1.522 (6)
N1—C8	1.456 (5)	C8—C10	1.556 (6)
N2—C14	1.327 (6)	C10—C11	1.509 (7)
N2—C12	1.366 (6)	C12—C13	1.351 (7)
O5—Zn01—N2	116.22 (13)	C2—C1—C6	117.4 (3)
O5—Zn01—N1	130.65 (13)	C3—C2—C1	121.2 (4)
N2—Zn01—N1	112.96 (13)	C2—C3—C4	121.5 (4)

O5—Zn01—O1	92.14 (12)	C5—C4—C3	118.1 (4)
N2—Zn01—O1	94.77 (12)	C4—C5—C6	122.5 (4)
N1—Zn01—O1	87.64 (11)	C5—C6—C1	119.2 (4)
O5—Zn01—O2	95.52 (13)	C5—C6—C7	116.4 (4)
N2—Zn01—O2	91.69 (14)	C1—C6—C7	124.2 (3)
N1—Zn01—O2	79.03 (12)	N1—C7—C6	125.5 (4)
O1—Zn01—O2	166.60 (11)	N1—C8—C9	109.2 (3)
C1—O1—Zn01	123.4 (2)	N1—C8—C10	108.0 (3)
C9—O2—Zn01	115.1 (3)	C9—C8—C10	108.7 (3)
C7—N1—C8	121.1 (3)	O3—C9—O2	124.9 (4)
C7—N1—Zn01	125.5 (3)	O3—C9—C8	117.8 (4)
C8—N1—Zn01	113.0 (2)	O2—C9—C8	117.2 (3)
C14—N2—C12	105.7 (4)	O4—C10—C11	110.5 (4)
C14—N2—Zn01	127.5 (3)	O4—C10—C8	107.7 (3)
C12—N2—Zn01	126.5 (3)	C11—C10—C8	112.3 (4)
C14—N3—C13	108.9 (5)	C13—C12—N2	110.8 (5)
O1—C1—C2	119.4 (3)	C12—C13—N3	104.6 (5)
O1—C1—C6	123.1 (3)	N2—C14—N3	110.0 (4)

Hydrogen-bond geometry (Å, º)

D—H···*A*	*D*—H	H···*A*	*D*···*A*	*D*—H···*A*
O4—H15···O2^{i}	0.79 (7)	1.89 (7)	2.678 (4)	170 (8)
O5—H16*A*···O1^{ii}	0.79 (7)	1.91 (7)	2.708 (4)	178 (6)
O5—H16*B*···O3^{i}	0.72 (8)	2.02 (8)	2.724 (4)	165 (7)
N3—H17···O1^{iii}	0.88	2.06	2.830 (6)	145
C14—H14···O2	0.95	2.61	3.077 (6)	111
C13—H13···O3^{iv}	0.95	2.36	3.253 (6)	156
C2—H2···O3^{v}	0.95	2.48	3.351 (5)	152

Symmetry codes: (i) −*x*+3/2, *y*−1/2, −*z*; (ii) −*x*+1, *y*, −*z*; (iii) *x*, *y*+1, *z*; (iv) *x*−1/2, *y*+1/2, *z*; (v) *x*−1/2, *y*−1/2, *z*.